

Accelerated Articles

## Nanoscale Atmospheric Pressure Laser Ablation-Mass Spectrometry

Raoul Stöckle,<sup>†</sup> Patrick Setz,<sup>†</sup> Volker Deckert,<sup>†</sup> Thomas Lippert,<sup>‡</sup> Alexander Wokaun,<sup>‡</sup> and Renato Zenobi<sup>\*,†</sup>

Department of Chemistry, Swiss Federal Institute of Technology (ETH) Zürich, Universitätstrasse 16, CH-8092 Zürich, Switzerland, and Paul Scherrer Institute, CH-5232 Villigen, Switzerland

**We describe an atmospheric pressure nanosampling interface for mass spectrometry based on near-field laser ablation. Pulsed laser radiation is delivered to the sample surface through a near-field optical probe, and the ablation plume is sampled through a capillary orifice and analyzed by standard MS methods. A spatial resolution of less than 200 nm and a sensitivity below 2 amol is demonstrated.**

Researching the nanometer scale is currently of great relevance in many branches of modern science and engineering, for example, in microelectronics, in supramolecular chemistry, or for understanding the function of complex biological “molecular machines” and subcellular compartments. Central to this task are powerful analytical tools that yield molecular information with nanometer spatial resolution. With this goal in mind, the scanning near-field optical microscope (SNOM)<sup>1</sup> has been developed from a mere variation of the scanning tunneling microscope into a useful analytical instrument for the nanoworld.<sup>2,3</sup> Of particular interest is the combination of SNOMs with spectroscopic methods, yielding detailed molecular information with a spatial resolution far better than that of the conventional optical microspectrometry. Fluorescence,<sup>4</sup> infrared,<sup>5</sup> and Raman spectroscopies<sup>6–8</sup> have been successfully combined with near-field optical microscopes, with

a resolution of less than 100 nm,<sup>9</sup> and a detection limit approaching that of a single molecule.<sup>10–12</sup>

Mass spectrometry (MS) has been enormously successful for chemical analysis of complex molecules, but MS has not been used in nanoscience and nanotechnology due to an intrinsic lack of spatial resolution of standard MS techniques. Spatially resolved analysis and MS imaging have become possible with laser microprobe mass spectrometers<sup>13,14</sup> and, more recently, using a MALDI imaging method.<sup>15</sup> However, the spatial resolution of the latter method is on the order of 25  $\mu\text{m}$ , and even the best laser microprobe instruments are limited to a resolution of a couple of micrometers. Elemental analysis can be carried out with somewhat higher spatial resolution, using secondary ion mass spectrometry (SIMS). A spatial resolution of as little as 60 nm has been achieved using dynamic SIMS, characterized by both high primary ion currents and a tightly focused beam, e.g., using  $\text{Ga}^+$  primary ions.<sup>16</sup> Molecular analysis on the submicrometer scale is much more difficult, because static SIMS, usually with a much less

\* To whom correspondence should be addressed. E-mail: zenobi@org.chem.ethz.ch.

<sup>†</sup> ETH Zürich.

<sup>‡</sup> Paul Scherrer Institute.

- (1) Pohl, D. W.; Denk, W.; Lanz, M. *Appl. Phys. Lett.* **1984**, *44*, 651–653.
- (2) Lewis, A.; Liebermann, K. *Anal. Chem.* **1991**, *63*, 625–638.
- (3) Zenobi, R.; Deckert, V. *Angew. Chem., Int. Ed.* **2000**, *39*, 1746–1756.
- (4) Betzig, E.; Trautman, J. K. *Science* **1992**, *257*, 189–195.
- (5) Knoll, B.; Keilmann, F. *Nature* **1999**, *399*, 134–137.
- (6) Stranick, S. J.; Richter, L. J.; Cavanagh, R. R. *J. Vac. Sci. Technol. B* **1998**, *16*, 1948–1952.

- (7) Smith, D. A.; Webster, S.; Ayad, M.; Evans, S. D.; Fogherty, D.; Batchelder, D. *Ultramicroscopy* **1995**, *61*, 247–252.
- (8) Deckert, V.; Zeisel, D.; Zenobi, R.; Vo-Dinh, T. *Anal. Chem.* **1998**, *70*, 2646–2650.
- (9) Stöckle, R.; Deckert, V.; Fokas, C.; Zeisel, D.; Zenobi, R. *Vibr. Spectrosc.* **1999**, *682*, 39–48.
- (10) Trautman, J. K.; Macklin, J. J.; Brus, L. E.; Betzig, E. *Nature* **1994**, *369*, 40–42.
- (11) Meixner, A. J.; Zeisel, D.; Bopp, M. A.; Tarrach, G. *Opt. Eng.* **1995**, *34*, 2324–2332.
- (12) Ruiter, A. G. T.; Veerman, J. A.; Garcia-Parajo, M. F.; van Hulst, N. F. *J. Phys. Chem. A* **1997**, *101*, 7318–7323.
- (13) van Vaeck, L.; van Roy, W.; Gijbels, R.; Adams, F. In *Laser Ionization Mass Analysis*; Vertes, A., Gijbels, R., Adams, F., Eds.; John Wiley & Sons: New York, 1993; Vol. 124, pp 7–126.
- (14) Zenobi, R. *Int. J. Mass Spectrom. Ion Processes* **1995**, *145*, 51–77.
- (15) Kooen, J.; Stöckli, M.; Caprioli, R. *J. Mass Spectrom.* **2000**, *35*, 258–264.
- (16) Benninghoven, A.; Hagenhoff, B.; Niehuis, E. *Anal. Chem.* **1993**, *65*, 630–640.

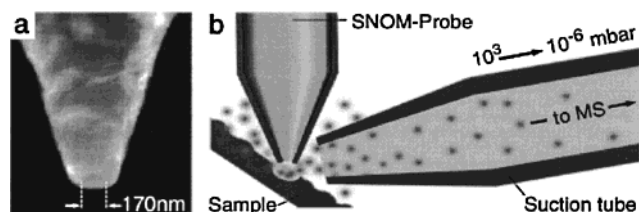


Figure 1. (a) Scanning electron micrograph of the tip of a near-field optical fiber probe used for laser ablation. Tips are produced by a chemical etching method<sup>23</sup> and subsequently metallized with aluminum. This production method ensures a large taper angle at the tip, resulting in high optical transmission (up to 1%) while maintaining small apertures ( $\sim 170$ -nm diameter in the present case). (b) Schematic diagram of the near-field laser ablation/nanosampling interface for mass spectrometry (not to scale).

focused primary ion beam, is employed;<sup>17,18</sup> experiments with submicrometer resolution remain exceptions.<sup>19</sup> For investigation by SIMS and other methods with high spatial resolution such as Auger electron microscopy, samples have to be kept at high vacuum. This complicates both their manipulation and visual inspection during analysis and is detrimental for biological samples. Similar problems were encountered by Kossakovski et al.,<sup>20</sup> who put an entire near-field laser ablation setup in a vacuum, in close proximity to a mass spectrometer ion source. A lateral resolution approaching  $1 \mu\text{m}$  was demonstrated by these authors, using acetylcholine deposited on a transmission electron microscopy grid as the sample.

The method reported here allows spatially resolved molecular analysis using mass spectrometry of specimens that are kept at ambient pressure. It relies on a combination of pulsed laser ablation through a near-field optical probe and atmospheric sampling of the ablated material through a capillary interface. The concept is shown schematically in Figure 1. If the tip is held very close to the sample surface, within a few nanometers, the illuminated area is essentially defined by the size of the aperture.<sup>21,22</sup> This permits material ablation from an area smaller than the Abbé barrier, the limit of resolution if diffractive optics is used ( $\sim 1/2$  of the incident laser wavelength). We have developed a method for producing near-field optical tips using a chemical etching method<sup>23</sup> with an exceptionally high optical transmission, up to 1%. These tips also feature a very high damage threshold, being able to withstand up to  $300 \mu\text{J}$  of laser pulse energy coupled into the fiber. The resulting power density under the tip aperture is high enough to effect desorption/ablation of solid material from a sample placed in the optical near field of the tip.<sup>24</sup> It has previously been demonstrated that a lateral resolution of  $70 \text{ nm}$  is possible for laser ablation through SNOM probes.<sup>24</sup>

(17) Van Vaeck, L.; Adriaens, A.; Gijbels, R. *Mass Spectrom. Rev.* **1999**, *18*, 1–47.

(18) Adriaens, A.; Van Vaeck, L.; Adams, F. *Mass Spectrom. Rev.* **1999**, *18*, 48–81.

(19) Benninghoven, A. *Surf. Sci.* **1994**, *299/300*, 246–260.

(20) Kossakovski, D.; O'Connor, S. D.; Widmer, M.; Baldeshwieler, J. D.; Beauchamp, J. L. *Ultramicroscopy* **1998**, *71*, 111–115.

(21) Synge, E. H. *Philos. Mag.* **1928**, *6*, 356–362.

(22) Hecht, B.; Sick, B.; Wild, U.; Deckert, V.; Zenobi, R.; Martin, O. J. F.; Pohl, D. W. *J. Chem. Phys.* **2000**, *112*, 7761–7774.

(23) Stöckle, R.; Deckert, V.; Fokas, C.; Zenobi, R.; Hecht, B.; Sick, B.; Wild, U. *P. Appl. Phys. Lett.* **1999**, *75*, 160–162.

(24) Dutoit, B.; Zeisel, D.; Deckert, V.; Zenobi, R. *J. Phys. Chem. B* **1997**, *101*, 6955–6959.

## EXPERIMENTAL SECTION

Laser ablation is achieved by a pulse from a frequency-tripled Nd:YAG laser (model PY61C-20, Continuum, Santa Clara, CA, 35-ps pulse width, 355-nm wavelength, up to  $250\text{-}\mu\text{J}$  pulse energy) coupled into the back end of a near-field optical fiber tip. Figure 1a shows an electron micrograph of the tip that was actually used in this study. This particular tip had a 170-nm-diameter aperture, creating laser ablation craters with about the same diameter (see below).

The interface consisted of a  $20\text{-}\mu\text{m}$ -i.d. stainless steel capillary welded to the tapered end of a 20-cm-long, 10-mm-i.d. stainless steel tube that was pointing directly toward the electron impact (EI) ionizer of a quadrupole mass spectrometer (QMS) (Leda Mass, Stoke-on-Trent, U.K.) ion source. The capillary inlet was positioned very close ( $<5 \mu\text{m}$ ) to the SNOM tip using a micro-actuator, and the sample was tilted toward the capillary for better sampling efficiency. The interface is essentially a controlled leak, which puts some demands on the vacuum pumps. With a 2000 L/s oil diffusion pump, we were able to maintain an operating pressure of better than  $5 \times 10^{-5}$  mbar in the main chamber, more than sufficient to operate the QMS. The mass spectrometer was either scanned to record complete mass spectra for identification of an ablated substance or preset to a known  $m/z$  value to follow the transient signal after an ablation laser pulse. The stainless steel tube could be heated to  $260 \text{ }^\circ\text{C}$  to prevent clogging of the orifice and prolonged adsorption of ablation products to its inner wall.

Anthracene was purchased from Sigma (Buchs, Switzerland) and used without further purification. Bis(phenyl-*N,N*-diethyltriazene) ether was synthesized according to a procedure described in the Ph.D. thesis of J. Stebani.<sup>25</sup>

## RESULTS AND DISCUSSION

Two strategies are possible for the combination of SNOM with MS detection, either ablation inside the mass spectrometer's ion source or placement of the SNOM outside the vacuum system. Mainly for practical reasons we chose the latter. A significant problem is to bring the tiny amount of ablated material into the ion source of the mass spectrometer. With an estimated crater size of  $200 \text{ nm}$  diameter  $\times$   $20 \text{ nm}$  depth, a volume of  $\sim 60\,000 \text{ nm}^3$  is ejected; i.e., a quantity of only  $\sim 1.7$  amol of organic substance must be efficiently transported through an interface into the ion source. The great advantage of this approach, however, is that samples can be easily handled, in principle even in a high pressure, corrosive, or reactive gas environment.

As an example, the analysis of an anthracene crystal surface is shown here. Molecular crystals are important in modern materials science; anthracene has previously been used for nanoscale patterning of polymers<sup>26</sup> and as dopant for laser-induced ablation of polymers.<sup>27</sup> In the latter case, a photothermal ablation mechanism has been suggested and anthracene was detected as intact molecule among the ablation products.<sup>28</sup> For the purpose of testing the direct sampling interface, focused laser radiation

(25) Stebani, J. Ph.D. Thesis, University of Bayreuth, Bayreuth, 1993.

(26) Gery, G.; Fukumura, H.; Masuhara, H. *J. Phys. Chem. B* **1997**, *101*, 3698–3705.

(27) Fukumura, H.; Mibuka, N.; Eura, S.; Masuhara, H.; Nishi, N. *J. Phys. Chem.* **1993**, *97*, 13761–13766.

(28) Fukumura, H.; Masuhara, H. *Chem. Phys. Lett.* **1994**, *221*, 373–378.

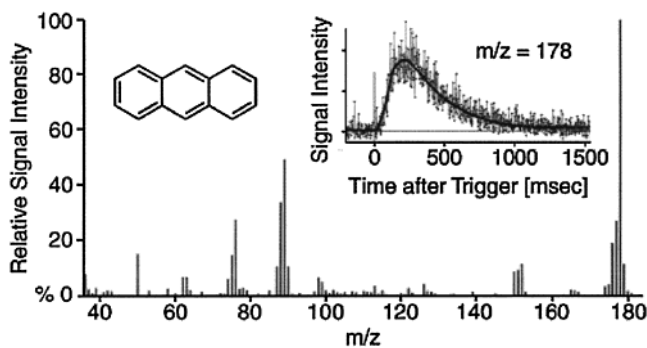


Figure 2. Mass spectrometric analysis of the ablation plume produced on the surface of an anthracene crystal by focused laser radiation. Peaks of the molecular ion ( $m/z$  178), a fragment  $M - C_2H_2$  ( $m/z$  152), and the doubly charged molecular ion ( $m/z$  89) allow identification of the compound. Inset: transient signal at  $m/z = 178$ . The line through the data points is drawn to guide the eye.

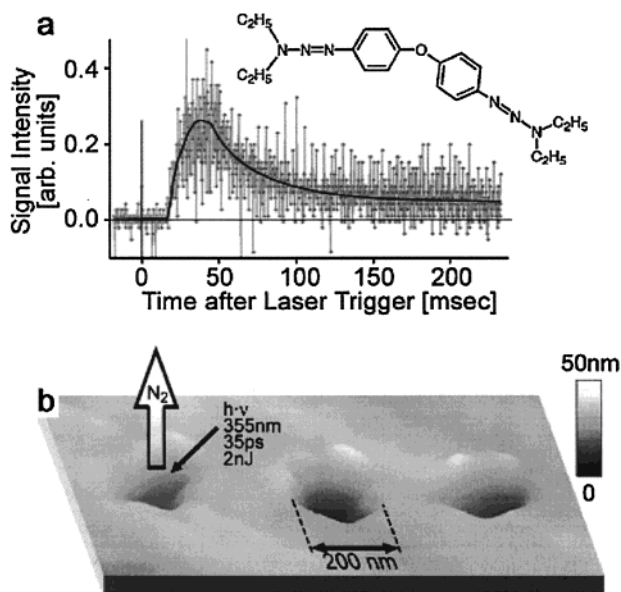


Figure 3. (a) Transient ablation signal of the decomposition product at  $m/z = 28$  (nitrogen) following near-field laser ablation from the surface of bis(phenyl- $N,N$ -diethyltriazene) ether (inset). (b) Topographic image of the surface of the triazene sample following the ablation experiment.

was used rather than a near-field tip, resulting in a larger crater size ( $\sim 5\text{-}\mu\text{m}$  diameter). The mass spectrum in Figure 2 is identical to that of anthracene, by comparison with electron impact ionization reference mass spectra.<sup>29</sup> The inset in Figure 2 shows that the anthracene signal appears after  $\sim 20$  ms and can be detected for up to 1 s, due to multiple adsorption/desorption processes on the walls of the interface tube.

Figure 3 demonstrates that the sensitivity of this setup is sufficiently high for individual near-field ablation events to be detected. The sample chosen for this experiment was a bis(phenyl- $N,N$ -diethyltriazene) ether. The bis(triazenes) are used as cross-linkers for aromatic polymers and fluorinated polyimides.<sup>30</sup> Triazenes are also applied as photochemically reactive dopants

in laser ablation of polymers.<sup>31,32</sup> Furthermore, the triazene chromophore is the crucial functional moiety of novel laser ablation photopolymers designed for direct structuring with specific excimer laser wavelengths, i.e., 308 and 355 nm.<sup>33,34</sup> The triazene groups absorb the laser energy and the polymers or molecules decompose into gaseous products. The most relevant product of laser-induced decomposition of triazenes is nitrogen, which acts as driving/carrier gas for ablation.<sup>33,34</sup> For this experiment, the QMS was therefore set to  $m/z = 28$ , the mass of nitrogen. To reduce the background signal from nitrogen in the atmosphere, and to avoid oxidizing the filament of the ion source, the sample was flooded with Ar. As shown in the upper part of Figure 3, a clear transient signal was observed for nitrogen, with an onset at 15 ms and lasting for  $\sim 200$  ms. Compared with the data in Figure 2 the time scale of this transient is shorter, due to the higher volatility and lower sticking coefficient of nitrogen compared with anthracene.

If a photochemical ablation process is indeed operative, as postulated for these materials,<sup>34</sup> desorption products should leave the sample during a shorter period of time than in the case of anthracene, where a photothermal mechanism<sup>24</sup> was shown to cause desorption, which is expected to result in evaporation over longer times. An estimate of the quantum yield for a photochemical decomposition of the bis(triazene) suggests that photochemical decomposition causes these craters. The estimation gives a quantum yield of  $2.8 \times 10^{-4}$ , assuming an energy of 2 nJ, a crater diameter of 200 nm with a depth of 20 nm, and a density of  $1\text{ g cm}^{-3}$ . The value of the quantum yield is quite comparable to the quantum yield of the photodecomposition of crystalline diphenyltriazene (DPT), i.e.,  $6 \times 10^{-4}$ ,<sup>35</sup> which has the same active chromophore. Further supporting the validity of this comparison, the quantum yield of decomposition of DPT in solution,  $10^{-3}$ – $2 \times 10^{-2}$ , depending on the solvent,<sup>36</sup> matches the range of  $1.8 \times 10^{-3}$ – $1.33 \times 10^{-2}$  reported for various aryldialkyl triazenes.<sup>37</sup> The detection of products by the mass spectrometer also strongly supports that material ablation is responsible for the observed craters, as opposed to indentations “written” into the sample surface thermomechanically, by transient elongation of the SNOM tip.<sup>38,39</sup>

The same numbers can be used to estimate the power density under the SNOM tip. With a pulse energy of 2 nJ exiting the tip ( $\sim 1\%$  transmission), a 200-nm aperture diameter, and a laser pulse width of 35 ps, we obtain a power density of roughly  $10^{11}\text{ W/cm}^2$ . This seems very high and may indeed be lower if a lower transmission is assumed and if losses due to coupling the laser into the back end of the fiber are greater. Presently, it is impossible

(29) Karcher, W. *Spectral Atlas of Polycyclic Aromatic Compounds*; Reidel: Dordrecht, The Netherlands, 1985; Vol. 1.

(30) Lau, A. K. N.; Vo, L. P. *Macromolecules* **1992**, *25*, 7294–7299.

(31) Lippert, T.; Wokaun, A.; Stebani, J.; Nuyken, O. *Angew. Makromol. Chem.* **1993**, *213*, 127–155.

(32) Lippert, T.; Yabe, A.; Wokaun, A. *Adv. Mater.* **1997**, *9*, 105–119.

(33) Lippert, T.; Stebani, J.; Ihlemann, J.; Nuyken, O.; Wokaun, A. *J. Phys. Chem.* **1993**, *97*, 12296–12301.

(34) Lippert, T.; Langford, S. C.; Wokaun, A.; Savas, G.; Dickinson, J. T. *J. Appl. Phys.* **1999**, *86*, 7116–7122.

(35) Baro, J.; Dudek, D.; Luther, K.; Troe, J. *Ber. Bunsen-Ges. Phys. Chem.* **1983**, *87*, 1161–1164.

(36) Baro, J.; Dudek, D.; Luther, K.; Troe, J. *Ber. Bunsen-Ges. Phys. Chem.* **1983**, *87*, 1155–1161.

(37) Lippert, T.; Stebani, J.; Nuyken, O.; Stasko, A.; Wokaun, A. *Photochem. Photobiol. A: Chem.* **1994**, *78*, 139–148.

(38) Hoen, S.; Mamin, H. J.; Rugar, D. *Appl. Phys. Lett.* **1993**, *64*, 267–269.

(39) La Rosa, A. H.; Yakobson, B. I.; Hallen, H. D. *Appl. Phys. Lett.* **1995**, *67*, 2597–2599.

to directly measure the pulse energy exiting the SNOM tip. However, such a power density is not unreasonable, either: Kossakovski and Beauchamp have recently demonstrated laser-induced breakdown spectroscopy with a lateral resolution in the micrometer range using uncoated tapered optical fiber tips.<sup>40</sup> These authors employed a nitrogen laser with a pulse width of 3 ns and estimated a power density of  $10^9$  W/cm<sup>2</sup> under their tip. Indeed, it cannot be excluded that a spark is ignited beneath our SNOM tip and that this may even be partially responsible for the ablation. We were not able to observe this directly, but if true, it may be possible to collect light from the area under the tip and thus to simultaneously obtain information on the elemental composition of the sample, by spectral analysis of the emission. However, damage of the SNOM tip, which may be expected for intense plasma conditions due to the laser pulse, has not been observed. In far-field ablation experiments, ablation is also found to occur before the power density for plasma formation is reached. Thus, we can currently only speculate about the existence and possible role of a plasma spark ignited under the SNOM tip.

#### CONCLUSIONS AND OUTLOOK

The analytical strategy described here differs from atmospheric pressure ionization mass spectrometry in that any ions produced in the near-field laser ablation step are ignored. Instead, we focus on the large excess of neutral molecules generated by the laser ablation process. They are transported into the vacuum and ionized by electron impact. We note that this is not a particularly efficient ionization method, and many possibilities exist to further improve the sensitivity of near-field laser ablation mass spectrometry. These include chemical ionization, photoionization, or other efficient, soft ionization methods. Mass analyzers that are better adapted to the particular challenges, such as ion traps or time-of-flight mass spectrometers operated at high repetition rate, should further lower the detection limit.

(40) Kossakovski, D.; Beauchamp, J. L. *Anal. Chem.* **2000**, *72*, 4731–4737.

Arguably, the detection of a fragment at  $m/z = 28$  in Figure 3 is not sufficient for mass spectrometric identification of the bis-(phenyl-*N,N*-diethyltriazeno) ether. However, Figure 2 clearly demonstrates that standard EI fragmentation patterns are obtained with the approach presented. The sensitivity and scanning speed of the QMS were not particularly well suited to detect fast transient signals of weaker peaks in the mass spectrum of bis(phenyl-*N,N*-diethyltriazeno) ether. Mass analyzers that are better adapted to the particular challenges should thus be used eventually, such as ion traps for ion accumulation or time-of-flight mass spectrometers operated at high repetition rate for achieving lower detection limits. Nevertheless, even with rather simple instrumentation we were able to demonstrate the feasibility of molecular nanosampling mass spectrometry at ambient pressure and with a spatial resolution of  $\leq 200$  nm.

We expect this method to become a useful tool in nanoanalytical science and technology. Many applications already exist that require nanoscale molecular analysis, for example, the study of individual submicrometer particles, characterization of heterogeneities in materials and on catalysts, and biological ultrastructures. Molecular mass spectrometry is a very powerful tool for chemical and structural analysis, and we have shown here how to extend its applicability into the nanometer regime.

#### ACKNOWLEDGMENT

We thank Drs. R. Knochenmuss and Y. D. Suh for stimulating discussion, and the Swiss National Science Foundation, National Research project "Nanotechnology" (NFP-36) for financial support of our work.

Received for review December 7, 2000. Accepted February 2, 2001.

AC001440B